On the YIG Film Filters

Makoto Tsutsumi, Kensuke Okubo

Faculty of Engineering and Design, Kyoto Institute of Technology,
Matsugasaki, Sakyo-ku, Kyoto 606, Japan

Abstract— A new type of YIG film filter is proposed which consists of a microstrip line with a substrate of YIG films sandwiched between two dielectric slabs. The dispersion and transmission characteristics are calculated numerically. A sharp stop band characteristics are observed experimentally with half-power bandwidth of 16.4 MHz. Alternatively, in the same line with an air gap band-pass characteristic is observed with quality factor of 430. These experimental results are discussed with theory.

I. Introduction

Yttrium Iron Garnet (YIG) film epitaxially grown on Gadolinium Gallium Garnet (GGG) substrate is an attractive medium for applications to microwave ferrite devices. Magnetostatic wave (MSW) devices using YIG film have been studied extensively to find high quality factor of resonators, and good tunability of filters and delay lines [1].

In these MSW devices shorted input and output transducers have been separately used in the YIG film waveguide, and magnetostatic approximation has been assumed for the analysis, which neglects the electric field.

This paper proposes a new type of YIG film waveguide, in which input and output ports are not separate but constructed in a microstrip line configuration on the YIG films. The stop and pass band filter characteristics of the microstrip line are demonstrated experimentally.

II. Theory

Fig. 1 shows the geometry of the problem. It consists of microstrip line on two YIG films grown epitaxially on both sides of GGG substrate and sandwiched between two dielectric slabs. The *dc* magnetic field H_0 is applied in the direction perpendicular to the plane of microstrip line. Since the thickness c of the substrate is very small compared to the wavelength, electromagnetic field can be assumed to be independent of the *dc* magnetic field in z direction. Thus field components E_z, H_x, and H_y are taken into consideration. Boundary condition of magnetic walls at both edges of the strip at $x = \pm\frac{w}{2}$ are also assumed to get the dispersion relation [2].

From Maxwell equations, Helmholtz equation for E_z can be derived in the GGG substrate and the dielectric slabs

$$\frac{\partial^2 E_z}{\partial x^2} + \frac{\partial^2 E_z}{\partial y^2} + \omega^2 \varepsilon_0 \varepsilon_r \mu_0 E_z = 0, \; \varepsilon_r = \begin{cases} \varepsilon_G \text{ ;in GGG} \\ \varepsilon_D \text{ ;in dielectric} \end{cases} \quad (1)$$

and in the YIG films

$$\frac{\partial^2 E_z}{\partial x^2} + \frac{\partial^2 E_z}{\partial y^2} + \omega^2 \varepsilon_0 \varepsilon \mu_0 \mu_{eff} E_z = 0 \, , \quad (2)$$

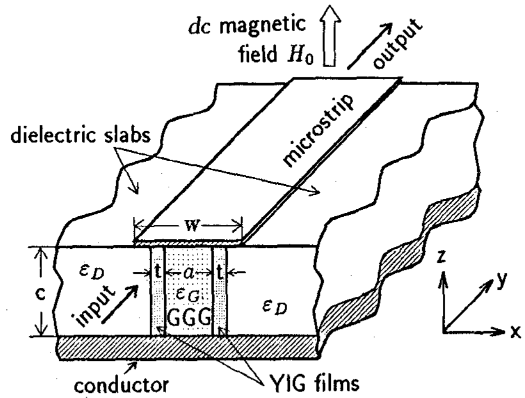

Fig. 1. Geometry of the problem.

where

$$\mu_{eff} = \frac{\mu^2 - \kappa^2}{\mu} \, ,$$

where μ and κ are the diagonal and off-diagonal coefficients of the permeability tensor which include magnetic loss as a function of ferrimagnetic resonance line width ΔH.

Solution of equations (1) and (2) are expressed as

$$E_z = (A_1 \sin \bar{\gamma}_x x + A_2 \cos \bar{\gamma}_x x) e^{-j\beta y} \quad \text{;in GGG} \quad (3)$$
$$E_z = (B_1 \sinh k_x x + B_2 \cosh k_x x) e^{-j\beta y} \quad \text{;in YIG} \quad (4)$$
$$E_z = C e^{-\gamma_x (x - \frac{w}{2})} e^{-j\beta y} \quad \text{;in dielectric} \quad (5)$$

where $\bar{\gamma}_x^2 = \omega^2 \varepsilon_0 \varepsilon_G \mu_0 - \beta^2$, $k_x^2 = \beta^2 - \omega^2 \varepsilon_0 \varepsilon \mu_0 \mu_{eff}$, $\gamma_x^2 = \beta^2 - \omega^2 \varepsilon_0 \varepsilon_D \mu_0$. A_1, A_2, B_1, B_2 and C are arbitrary constants and β is the propagation constant in y direction.

Matching tangential electromagnetic fields E_z and H_y at the boundaries $x = \pm\frac{a}{2}$, $\pm(\frac{a}{2} + t)$ and assuming magnetic wall of $H_y = 0$ at $x = \pm\frac{w}{2}$, the homogeneous equation in the matrix form with arbitrary constants is obtained, and by making its determinant to zero, dispersion relation is derived.

Fig. 2 shows typical dispersion curve for real part of the propagation constant estimated numerically from dispersion relation. The material parameters are depicted in the inset of the figure. The dispersion curve is almost same as that of TEM mode except around the frequency $f_r = \frac{\gamma \mu_0}{2\pi} \sqrt{H_0 (H_0 + M)}$.

Fig. 3. shows enlarged dispersion curve of complex propagation constant near f_r. Phase constant shown in Fig. 3(a) shows mixed curves of quasi-TEM mode and magnetostatic surface wave mode (MSSW). Attenuation constant α shown in Fig. 3(b) changes abruptly at f_r.

CH3141-9/92/0000-1397$01.00 © 1992 IEEE

To confirm the effect of substrate thickness $c = 2$ mm, dispersion relation under magnetostatic approximation has been estimated under three dimensional analysis, and is shown as dotted lines in Fig. 3. It is noted that dotted lines coincide with the solid lines in the case of electromagnetic field analysis of two dimensions except for dispersion curve of quasi-TEM mode.

Transmission characteristics of the waveguide in terms of scattering parameters are estimated theoretically based on the numerical values of dispersion curves of Figs. 2 and 3, and with characteristic impedance defined by

$$Z_0 = \frac{\int_{-\frac{w}{2}}^{\frac{w}{2}} E_z dx}{\int_{-\frac{w}{2}}^{\frac{w}{2}} H_x dx}. \tag{6}$$

Transmission coefficient of S_{21} for line length of 10 mm at C band are estimated numerically for two different ΔH values, and shown in Fig. 4. It can be seen from figure that S_{21} depends strongly on the ΔH values. Sharp notch characteristic is found around $f_r = 8$ GHz, where strong interaction between quasi-TEM and MSSW modes occurs for $\Delta H = 0.5$ Oe.

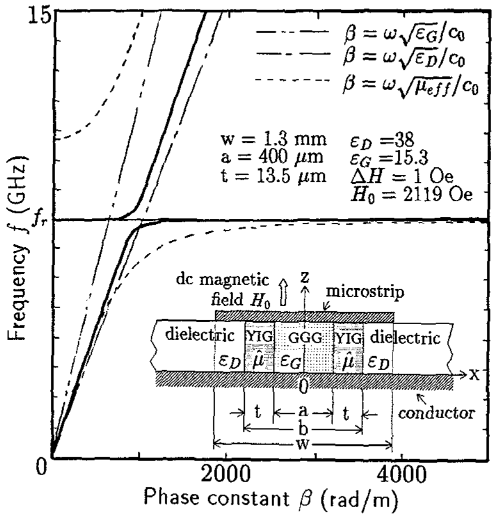

Fig. 2. Dispersion diagram.

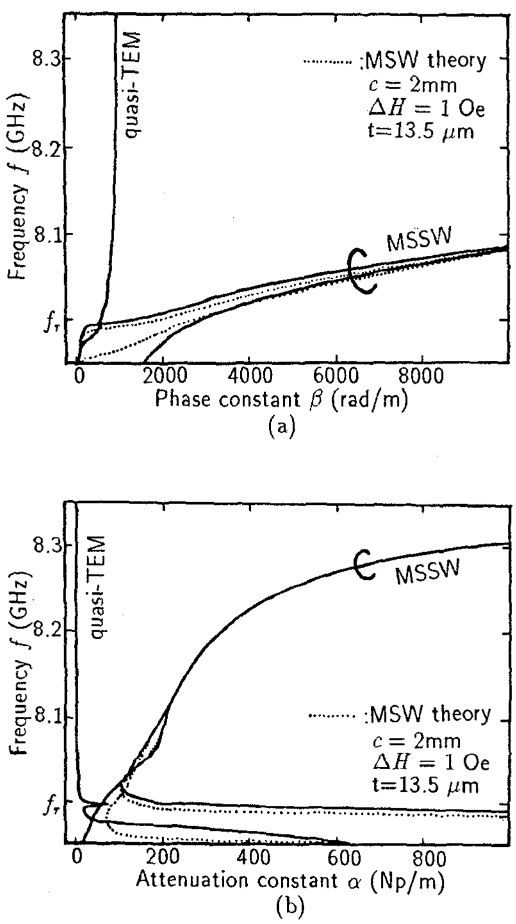

Fig. 3. Comparison between dispersion curve of electromagnetic and magnetostatic modes. (a) phase constant, (b) attenuation constant.

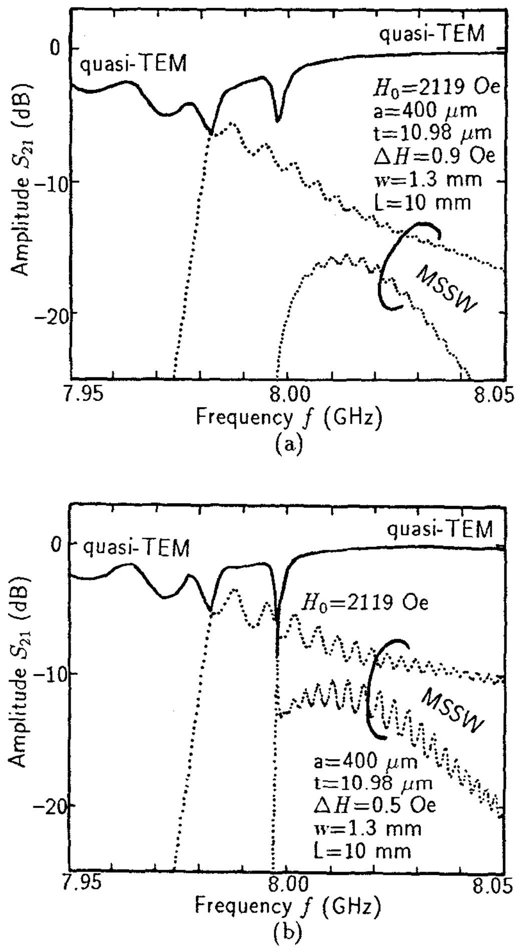

Fig. 4. Transmission characteristics of the line. (a) $\Delta H = 0.9$ Oe, (b) $\Delta H = 0.5$ Oe.

III. Experiment

The basic experimental configuration of the line is shown in Fig. 5. It consists of YIG films of dimensions 2 × 10 mm^2 with 10.98 μm thickness grown epitaxially on GGG of thickness 400 μm and the ferrimagnetic resonance line width ΔH of 1 Oe. To concentrate *RF* energy under the microstrip line, YIG-GGG-YIG films are sandwiched between two high dielectric ceramic slabs of ε_D=38 and dimension of 5 × 2 × 10 mm^3. A magnetic field H_0 is applied normal to the plane of microstrip line. Thus MSSW will be excited by the electric field of quasi-TEM mode in the microstrip line, which is effective in the near cut off region of MSSW and in a narrow bandwidth.

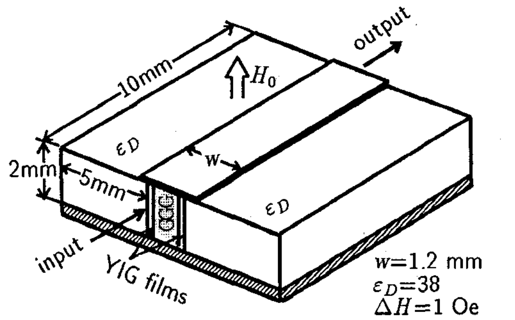

Fig. 5. Experimental configuration of band-stop filter.

The width of the microstrip is adjusted to match 50 Ω impedance of *RF* source and to obtain good filter characteristic at *C* band.

A typical transmission characteristic of the line is shown in Fig. 6. A sharp stop band characteristic is observed with 3 dB bandwidth of 16.4–23.1 MHz, maximum attenuation of ~25 dB, and insertion loss of ~1.4 dB in the frequency range

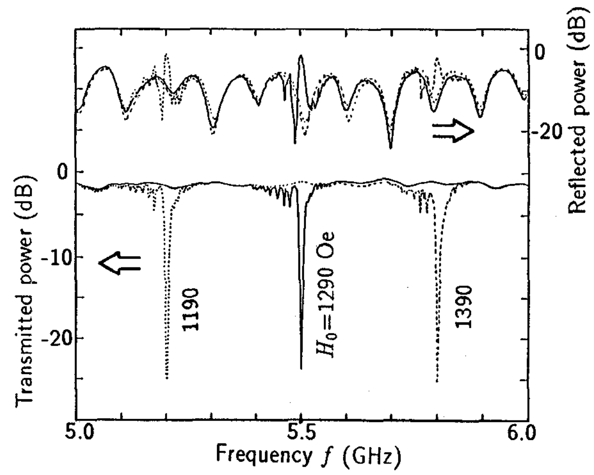

Fig. 6. Measured frequency response of band-stop filter.

of 5 GHz to 6 GHz, which is in similar performance as predicted from theory in Fig. 4. The quality factor of Q_e=335 can be read from figure at resonance frequency of 5.5 GHz. However it is experimentally found that the resonance frequency can be tuned up to 8 GHz with few dB insertion loss by the bias magnetic field, but beyond 7 GHz the filter characteristics are degraded with large ripples. In another study, the microstrip line on YIG film substrate which was reported in [3] has wider bandwidth with large ripples.

Next, a gap of 0.8 mm width is fabricated in the center of the microstrip line to cut off the quasi-TEM mode and to allow the MSSW mode to pass through the gap as shown in Fig. 7. Using the line with air gap the band-pass characteristic observed is shown in Fig. 8. It can be seen that the quality factor Q_e is ~430 with insertion loss of ~2.6 dB but spurious response of the filter is found below 20 dB.

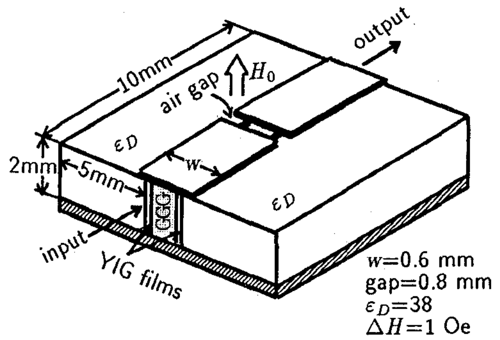

Fig. 7. Experimental configuration of band-pass filter.

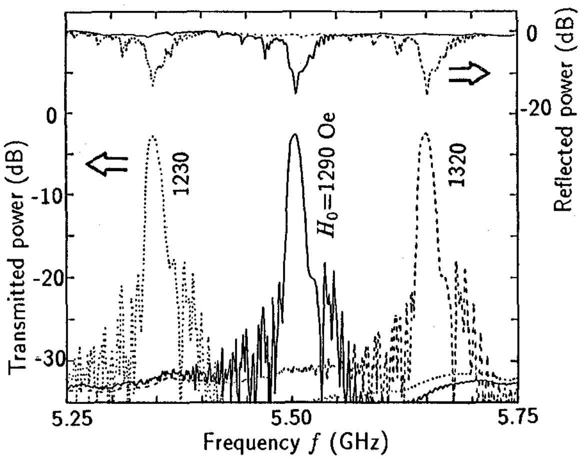

Fig. 8. Measured frequency response of band-pass filter.

Filter characteristics of microstrip line of multi layered YIG film are examined. Two cells of YIG-GGG-YIG films sandwiched between ceramic slabs are used as substrate and its stop and pass band characteristics are shown in Figs. 9 and 10. It can be seen from figures that sharp notch characteristics of filter is reduced with large ripples and that

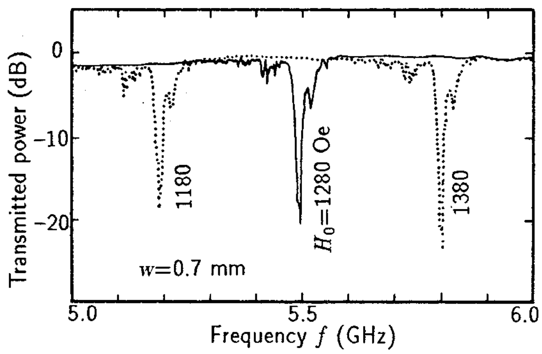

Fig. 9. Measured frequency response of band-stop filter for two cells of YIG-GGG-YIG films.

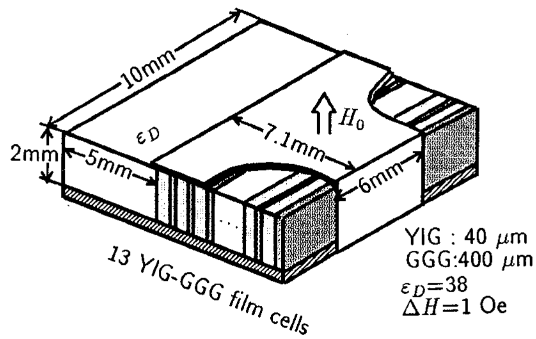

Fig. 11. Experimental configuration of edge guide isolator.

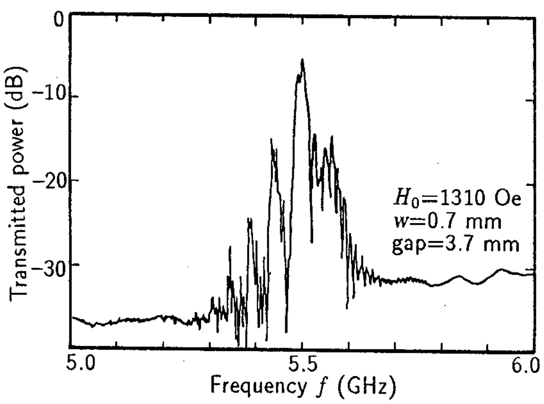

Fig. 10. Measured frequency response of band-pass filter for two cells of YIG-GGG-YIG films.

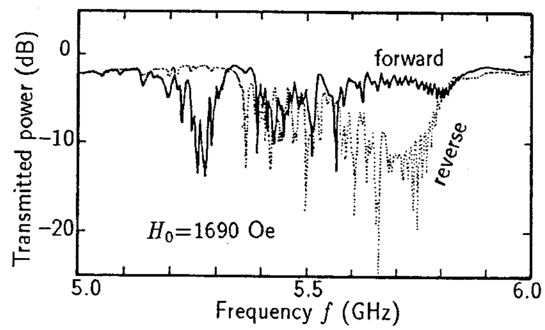

Fig. 12. Edge guide isolator characteristic.

dynamic range of pass band filter characteristic is also reduced with many spurious responses. These ripples and spurious responses may be due to the multiple coupling between MSSWs propagating through each YIG films.

Finally the edge-guided mode isolator using thirteen cells of YIG-GGG films was fabricated. The 10 dB isolation ratio is found in a narrow bandwidth as shown in Fig. 12.

IV. Conclusions

A new YIG film microstrip line has been studied and its filter characteristics are experimentally observed . It has an advantage to give both stop and pass band characteristics in the same line structure. If we use the waveguide of the multi layered structure of thin YIG film less than 10 μm, filter characteristics could be further improved, and might find another application such as edge-guided mode isolator.

Acknowledgment

This work has been supported by Japan Broadcasting Foundation 1990, and we thank to Murata Mfg. Co., Ltd. for technical assistance.

References

[1] "Special section on microwave magnetics", *Proc. IEEE*, vol. 76, pp. 121-200, Feb. 1988.

[2] M.E. Hines: "Reciprocal and nonreciprocal modes of propagation in ferrite stripline and microstrip devices", *IEEE Trans. Microwave Theory Tech.*, vol. MTT-19, pp. 442-451, May 1971.

[3] M. Tsutsumi and T. Asahara: "Microstrip lines using Yttrium Iron Garnet Film", *IEEE Trans. Microwave Theory Tech.*, vol. MTT-38, pp. 1461-1467, Oct. 1990.